

On the Interpolation of Model Atmospheres and High-Resolution Synthetic Stellar Spectra

Sz. Mészáros^{1,2}, C. Allende Prieto^{1,2}

ABSTRACT

We present tests carried out on optical and infrared stellar spectra to evaluate the accuracy of different types of interpolation. Both model atmospheres and continuum normalized fluxes were interpolated. In the first case we used linear interpolation, and in the second linear, cubic spline, cubic-Bezier and quadratic-Bezier methods. We generated 400 ATLAS9 model atmospheres with random values of the atmospheric parameters for these tests, spanning between -2.5 and $+0.5$ in $[\text{Fe}/\text{H}]$, from 4500 to 6250 K in effective temperature, and 1.5 to 4.5 dex in surface gravity. Synthesized spectra were created from these model atmospheres, and compared with spectra derived by interpolation. We found that the most accurate interpolation algorithm among those considered in flux space is cubic-Bezier, closely followed by quadratic-Bezier and cubic splines. Linear interpolation of model atmospheres results in errors about a factor of two larger than linear interpolation of fluxes, and about a factor of four larger than high order flux interpolations.

1. Introduction

Even within the framework of classical LTE 1D models, the calculation of a stellar model atmosphere takes a finite amount of time, which can be significant when complex opacities are involved. Massive spectroscopic surveys require large numbers of models spanning a wide range of parameters and can become very time consuming. Depending on the algorithm used, even the analysis of a single star may require many model atmospheres to evaluate the performance of different combinations of parameters.

In practice, the need for model spectra for many parameter combinations is satisfied by taking one or several shortcuts that avoids the actual calculation of self-consistent models. The most wide-used strategy is some sort of interpolation, either in the model atmosphere (the run with height of the main thermodynamical variables), or in the emerging radiative fluxes or intensities. Different recipes have been used, and codes circulate among researchers, but few have been published and thoroughly tested.

¹Instituto de Astrofísica de Canarias (IAC), E-38200 La Laguna, Tenerife, Spain

²Departamento de Astrofísica, Universidad de La Laguna (ULL), E-38206 la Laguna, Tenerife, Spain

In this paper we perform a battery of tests in order to quantify the typical errors incurred when interpolating model atmospheres or the model fluxes calculated from them. Section 2 describes our calculations and §3 our results, with a summary provided in §4.

2. Calculations

We generated a regular grid of ATLAS9 model atmospheres with $[\text{Fe}/\text{H}]$ from -2.5 to $+0.5$ in steps of 0.5 dex, T_{eff} from 4500 K to 6250 K in steps of 250 K, and $\log g$ from 1.5 to 4.5 dex in steps of 0.5 dex. We also calculated 400 additional models with random parameters within the boundaries of the regular grid. The microturbulence was chosen to be constant at 2 km s^{-1} in all our calculations.

The relatively small range of T_{eff} is to ensure that all ATLAS9 models are fully converged throughout the entire atmosphere. Since ATLAS9 start to experience convergence problems in the outer layers of the atmosphere below 4250 K and above $\log g = 4$, especially at low metallicities, we chose to omit that region from the calculations. Stars warmer than 6250 K have spectra dominated mainly by hydrogen lines, thus it is expected that interpolation errors will decrease as temperatures increase, and the examples of spectra with 6250 K are good representation of warmer stars. After careful consideration we decided that the above values gave the largest range in all three parameters combined.

Two representative wavelength regions were chosen, one in the optical, and including both weak and strong spectral lines (the Mg *Ib* triplet) between 516.5 and 519.5 nm, and one in the near-infrared, and in particular the H-band window, targeted by the Apache Point Galactic Evolution Experiment (APOGEE, Allende Prieto et al. 2008; Eisenstein et al. 2011; Wilson et al. 2012), spanning between 1509.1 and 1699.5 nm.

We carried out two types of tests, one involving interpolation in the model atmospheres directly, and a second one involving interpolation in the emergent fluxes. In the first type of test, we interpolated models with the chosen random parameters from the grid, and synthesized the emergent spectra. The comparison was made between these and the fluxes calculated from the models with the randomly generated parameters.

In the second case, we calculated the emergent spectra for the models generated from the random parameters (true flux), and the evenly distributed models. Then, we interpolated the spectra from the evenly spaced models to the sets of random parameters and examined the differences in continuum normalized flux relative to the true flux. The flux interpolation tests were performed with linear (F(L)), cubic spline (F(CS)), cubic-Bezier (F(CB)), and quadratic-Bezier (F(QB)) methods, while in the case of the model atmosphere interpolations (MA) we only explored the linear algorithm.

2.1. Model atmosphere calculations

Our regularly spaced ATLAS9 model atmospheres were calculated as described by Meszaros et al. (2012). However, there are some differences between these models and those presented by Meszaros et al. (2012)¹: those used here correspond to different versions of the line data, and an older version of the code, plus a number of other differences regarding the configuration of the input for the ATLAS9 code. The calculations used here are older, and the updated ones are to be preferred, but since these details are irrelevant for the evaluation of the interpolation accuracy, we have chosen to retain the custom-made calculations.

The opacity distribution functions (ODFs) and Rosseland opacities needed as input were calculated using the DFSYNTH and KAPPA9 codes, while the model atmospheres were generated with the linux version of the ATLAS9 code (Kurucz 1979, 1993; Sbordone 2004, 2005). The ODF calculations followed the method described by Castelli & Kurucz (2003); Castelli (2005), while the model atmosphere calculations are detailed in Meszaros et al. (2012). ATLAS9 gives excellent convergence in the parameter range chosen above.

In addition to the regular grid, we made calculations for 400 additional random models. The parameters for these were drawn from random uniform distributions across the chosen ranges. These calculations are fully consistent with the models in the grid.

2.2. Model atmosphere interpolation

We interpolated model atmospheres for the 400 sets of random parameters. For each target model, we identified the 8 immediate neighbors with higher and lower values for each parameter in the grid, calculated by numerical integration the Rosseland optical depth for each, re-sampled all the thermodynamical quantities in the atmosphere (temperature, gas pressure, and electron density) on a common optical depth scale for all models by linear interpolation, and then interpolated, linearly, all the thermodynamical quantities to the parameters (T_{eff} , $\log g$, and $[\text{Fe}/\text{H}]$) of the target model.

Other quantities included in the models (Rosseland opacities, radiative pressure, etc.) were also interpolated in the same way. The interpolations were carried out using the `kmod` code. This code has already been used in a number of investigations (Reddy et al. 2003, 2006; Yong et al. 2013). It is written in IDL and it is publicly available².

¹<http://www.iac.es/proyecto/ATLAS-APOGEE/>

²<http://leda.as.utexas.edu/stools>

2.3. Calculation of model fluxes

We calculated model fluxes for all model atmospheres using the ASSeT spectral synthesis code (Koesterke et al. 2008; Koesterke 2009) with detailed continuum opacities by Allende Prieto et al. (2003) and updates from Allende Prieto (2008). Line data come mainly from the calculations and compilations by Kurucz (available from his website³), enhanced with damping constants from Barklem (2007) when available.

We adopted solar reference abundances as in Asplund et al. (2005), and the compositions used in the calculations of the model atmospheres were consistent with those adopted in the spectral synthesis. We underline, however, that the interpolation tests performed here are fairly insensitive to the particular choices for the reference solar composition and the atomic and molecular data, as long as these choices are reasonable and lead to spectra that resemble approximately the modeled stars. The most critical aspect, is to ensure that the calculations for the models in the grid and those with random parameters used for tests, are completely consistent.

2.4. Flux Interpolations

Flux interpolations are consecutively performed in surface gravity, effective temperature, and metallicity. Quadratic and cubic Bezier interpolation are implemented with control values that make the algorithm identical to Hermite interpolation, and therefore both the interpolating function and its derivatives are continuous. In the case of cubic Bezier interpolation, quadratic Bezier interpolation was forced for those dimensions for which the target parameters were in the intervals adjacent to the edges of the grid.

The Bezier interpolations were implemented afresh in the FORTRAN spectral fitting code FERRE (Allende Prieto 2006) following the description by Auer (2003) and references therein. Cubic splines interpolation was included calling a subroutine from the library provided with the book by Chapman (2004), which follows the discussion given in Press et al. (1992).

3. Discussion

Before examining the errors in the fluxes, we compared interpolated model atmospheres with the calculated ones. The linear interpolation does a good job at estimating the real atmospheric structure; the temperature differences were between 2 – 3%, the pressure and electron density differences were between 1 – 2%. This translates to 10–30 K average differences in temperature in case of cool atmospheres above $\log \tau_{Ross} < 1$, from where all of the spectral lines form. This difference slightly increases as the effective temperature gets higher.

³<http://kurucz.harvard.edu/>

To measure the amount of error each interpolation method makes, we calculated the same statistics for each case. In the case of absolute fluxes, we only examined the average differences throughout the whole wavelength range, to track how much the continuum level changes. In the case of optical spectra, the atmosphere interpolation gives 1–5% smaller continuum levels than the direct calculations, and we find that the linear flux interpolation gives -0.3–+0.5% relative differences, usually shifted slightly higher than the true continuum in case of the optical spectrum, but not in the infrared. The errors are smaller in the IR region, 0.5–+1% in the continuum level when atmospheres are interpolated and 0.01–0.1% with linear interpolation in flux.

Two examples of the differences between interpolated and direct calculations of continuum normalized spectra are given in Figures 1 and 2. Figure 1 shows a metal-poor G-type giant, while Figure 2 shows a metal rich, K-type dwarf – these two cases represent the extremes of our parameters space. The metal-poor spectra only show large differences in the line cores. The average error can be up to 1% in the optical and infrared metal-poor warm spectrum, while in case of the metal-rich cool spectrum this goes up to 5–10% in the optical and 1–2% in the infrared. The differences in the line profile for the cooler atmosphere increase by a factor of 4 in both wavelength regions compared to the metal-poor case due to weak atomic metal and molecular lines very sensitive to small temperature changes in the atmosphere. In the infrared spectra of the G-type metal-poor star, the differences are dominated by the hydrogen Brackett lines, while in the optical these are associated with the magnesium triplet lines. This picture changes dramatically in case of the metal-rich, cool dwarf (Figure 2), where the Brackett lines disappear and the "noise" increases greatly in the continuum of the IR spectrum due to weak atomic and molecular lines (CN, OH, and CO). Also, relative errors in the line cores are significantly higher than near the continuum.

To measure the overall performance of the interpolation methods across the parameter range, the differences respect to the true fluxes were calculated at each wavelength in the continuum normalized spectra. The average, standard deviation and maximum deviation above and below the continuum in the whole wavelength range were determined. The last two of these three parameters track different aspects of the error distribution. The standard deviation gives an estimate of the overall changes in the full flux range, while the maximum deviation shows mainly the differences in the line cores, where errors tend to be largest. The differences vary depending on where one samples the spectrum: they are small in the continuum, but typically larger in the line cores.

Figure 3 illustrates how the average differences depend on metallicity, effective temperature and gravity. The errors, both the average errors and the standard deviation, grow with increasing metallicity and decreasing temperature, but they do not depend so much on surface gravity. These correlations are easily understood as a result of an increased number of molecular and atomic absorption lines appearing in the spectrum at high metallicity and low temperature.

Both in the model atmosphere and linear flux interpolation methods, it is clearly visible that errors are significantly enhanced for values of the metallicity half way between the nodes of the grid. The evenly distributed models spanned -2.5 to $+0.5$ in $[\text{Fe}/\text{H}]$ with steps 0.5, and in the

vicinity of these values the linear interpolation gives significantly lower errors. Using higher order interpolations makes this effect to disappear. None of the methods is sensitive to this issue along the axis for effective temperature (nodes spaced every 250 K) or $\log g$ (nodes every 0.5 dex).

The overall results for each test are listed in Table 1 and illustrated in Figure 4. In the optical, the average differences are about $0.17 \pm 0.19\%$ for the case of MA interpolation, and smaller than 0.07% for all the interpolations in flux. The standard deviation of the relative differences paints a more dramatic picture. The MA method clearly shows the largest deviation up to 1% near the continuum level in the optical and, while F(CB) is the most accurate method with only 0.1% errors. In the infrared all interpolation methods perform well giving much smaller errors than in the optical, close to an average of $0-0.02\%$ differences. The scatter is about four times larger in the case of MA than in any other methods in both optical and infrared.

Figure 5 shows the maximum deviation of differences below and above the continuum level in the case of the cubic-Bezier interpolation. At optical wavelengths, the differences are generally higher than in the infrared, but they are usually smaller than 0.01 in ΔF ($1-2\%$). While a reduction of the errors near the grid nodes was not visible in the average differences, here it is apparent as a function of metallicity below $[\text{Fe}/\text{H}] = -1$, and the effect increases as $[\text{Fe}/\text{H}]$ decreases. The interpolation gives the highest errors in the line cores, i.e. in the highest atmospheric layers the spectrum is sensitive to.

4. Conclusions

We conclude that if model spectra need to be interpolated, the best way to proceed, among those explored, is to use high-order interpolation in continuum-normalized fluxes. Linear interpolation of model atmospheres leads to about a factor of $3-5$ higher error than high order interpolations in flux, at about $-0.17 \pm 0.19\%$ average differences in the optical, and $0.0004 \pm 0.038\%$ in the infrared. Linear interpolation in flux space gives a factor of two smaller errors than using model atmospheres, but there is still a factor of two improvements found using high order functions. The most accurate flux interpolation method is cubic-Bezier with average errors of $0.011 \pm 0.047\%$ in the optical and $0.0011 \pm 0.0075\%$ in the infrared for our grids and random parameters. The cubic spline and quadratic-Bezier interpolations lead to only marginally higher errors than this. We conclude that interpolation errors become visible at $S/N = 10-20$ in the line cores in case of model atmosphere interpolations in the optical, and at $S/N = 20-40$ in the infrared, while the errors from cubic-Bezier flux interpolation will only show up above $S/N \sim 100-200$ in both wavelength ranges.

We must stress that only one code for the interpolation of model structures has been tested. Other codes with somewhat different strategies could provide somewhat different performances. We have allowed our high-order interpolations in flux to get to any value, even if artificial extrema are created (see the discussion by Auer 2003).

Our tests are restricted to stars with spectral types roughly between F5 and K5. Nevertheless,

we expect that the tendencies seen in our study will persist outside this domain. For example, we expect that errors will continue to reduce for the interpolation of stars with warmer temperatures, and to increase at temperatures under 4500 K.

Our analysis includes only linear and polynomial interpolation, but more sophisticated schemes are available and their performance could be somewhat different. Further work dealing with principal component analysis (PCA), neural networks, and other algorithms would be a natural followup of this investigation.

We would like to thank our colleagues at the SDSS-3 APOGEE survey for providing continuous discussions on various interpolation techniques. We greatly appreciate the contribution of Lars Koesterke on spectral synthesis with the ASS ϵ T code. We are also grateful for the referee for his helpful suggestions.

REFERENCES

- Allende Prieto, C., Beers, T. C., Wilhelm, R., Newberg, H. J., Rockosi, C. M., Yanny, B. & Lee, Y. S. 2006, *ApJ*, 636, 804
- Allende Prieto, C. 2008, *Physica Scripta Volume T*, 133, 014014
- Allende Prieto, C., Majewski, S. R., Schiavon, R., Cunha, K., Frinchaboy, P., Holtzman, J., Johnston, K., Shetrone, M., Skrutskie, M., Smith, V., & Wilson, J. 2008, *AN*, 329, 1018
- Allende Prieto, C., Lambert, D. L., Hubeny, I., & Lanz, T. 2003, *ApJS*, 147, 363
- Asplund, M., Grevesse, N. & Sauval, A. J. 2005, *ASPC*, 336, 25
- Auer, L. 2003, in *Stellar Atmosphere Modeling*, I. Hubeny, D. Mihalas and K. Werner, eds., *ASP Conf. Series*, 288, p3–15
- Barklem, P. S. 2007, *A&A*, 466, 327
- Castelli, F. 2005, *MSAIS*, 8, 344
- Castelli, F., & Kurucz, R. L. 2003, *New Grids of ATLAS9 Model Atmospheres*, *IAUS*, 210, 20P
- Chapman, S. J. 2004, *Fortran 90/95 for scientist and engineers*, 2nd edition, McGraw-Hill
- Eisenstein, D.J., et al. 2011, *AJ*, 142, 72
- Koesterke, L. 2009, *American Institute of Physics Conference Series*, 1171, 73
- Koesterke, L., Allende Prieto, C. & Lambert, D. L. 2008, *ApJ*, 680, 764
- Kurucz, R. L. 1979, *ApJS*, 40, 1

- Kurucz, R. L. 1993, ATLAS9 Stellar Atmosphere Programs and 2 km s⁻¹ grid. Kurucz CD-ROM No. 13. Cambridge, Mass.: Smithsonian Astrophysical Observatory, 1993, 13
- Meszáros, Sz., Allende Prieto, C., Edvardsson, B., Castelli, F., García Pérez, A. E., Gustafsson, B., Majewski, S. R., Plez, B., Schiavon, R., Shetrone, M., & de Vicente, A. 2012, *AJ*, 144, 120
- Press, W. H., Teukolsky, S. A., Vetterling, W. T., Flannery, B. P. 1992, *Numerical Recipes in Fortran 77: the art of scientific computing*, 2nd edition, Cambridge Univ. Press
- Reddy, B. E., Lambert, D. L. & Allende Prieto, C. 2006, *MNRAS*, 367, 1329
- Reddy, B. E., Tomkin, J., Lambert, D. L. & Allende Prieto, C. 2003, *MNRAS* 340, 304
- Sbordone, L. 2005, *MSAIS*, 8, 61
- Sbordone, L., Bonifacio, P., Castelli, F., & Kurucz, R. L. 2004, *MSAIS*, 5, 93
- Wilson, J. C. et al. 2012, *SPIE*, 8446, 0
- Yong, D. et al. 2013, *ApJ*, 762, 26

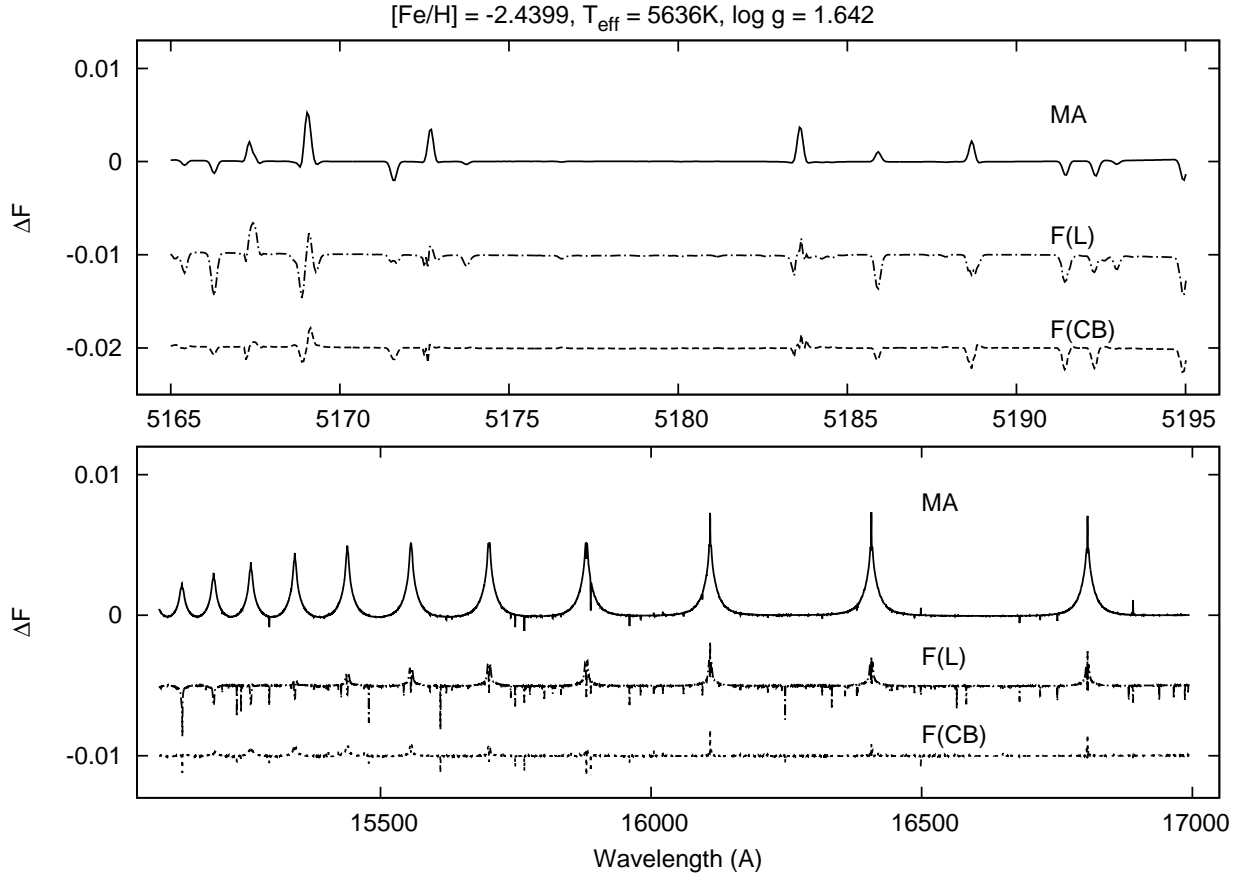


Fig. 1.— Examples of differences of continuum normalized spectra in case of a metal-poor hot giant. On the left panels relative differences, while on the right side normal differences compared to the true flux are shown. Only three interpolation methods are presented: model atmosphere (MA), linear flux F(L), and cubic-Bezier flux F(CB). F(L) and F(CB) are shifted down by 0.01 and 0.02 respectively in the optical, and by 0.005 and 0.01 in the infrared spectrum to aid visibility. The MA method gives the largest errors, while F(CB) shows the smallest differences.

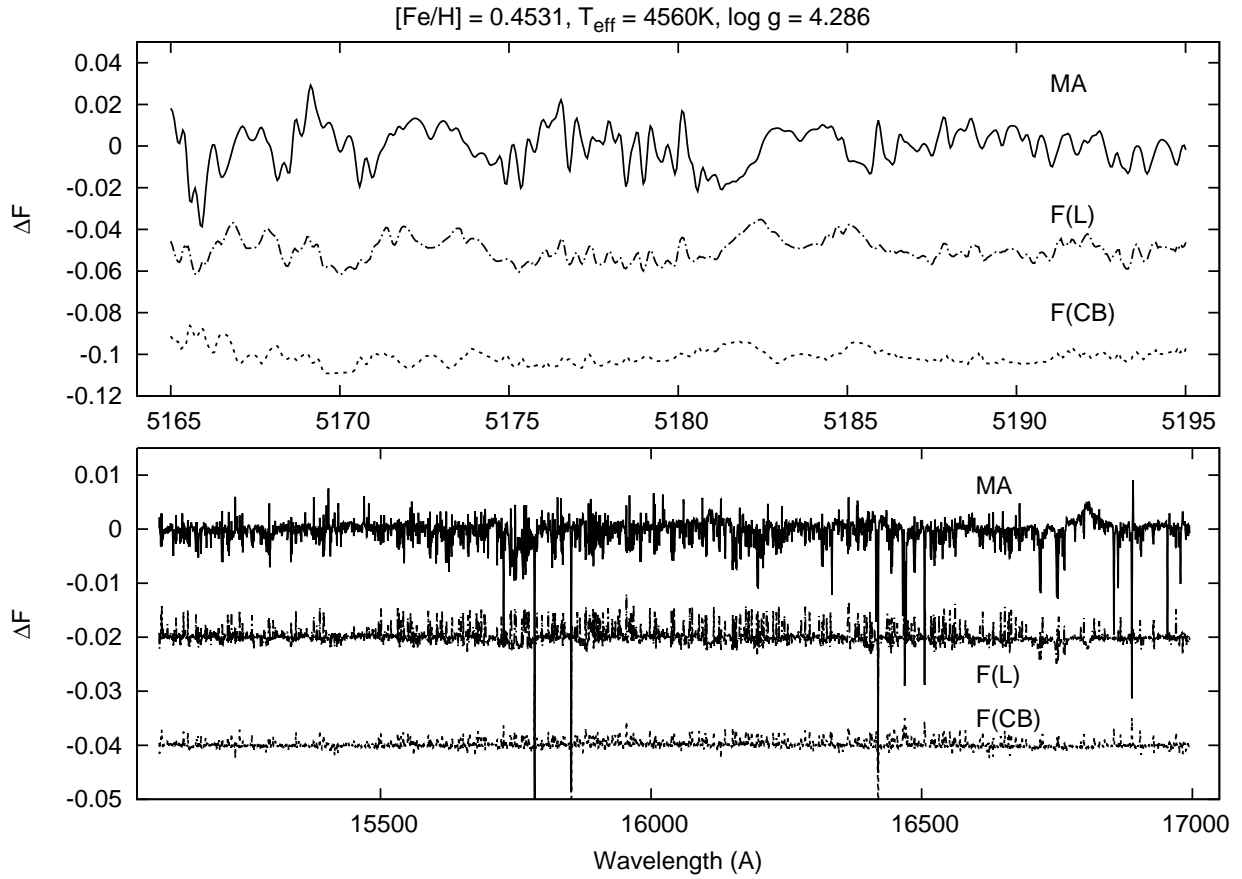


Fig. 2.— Examples of differences of continuum normalized spectra in case of a metal-rich cool dwarf. F(L) and F(CB) are shifted down by 0.05 and 0.1 respectively in the optical, and by 0.02 and 0.04 in the infrared spectrum to aid visibility.

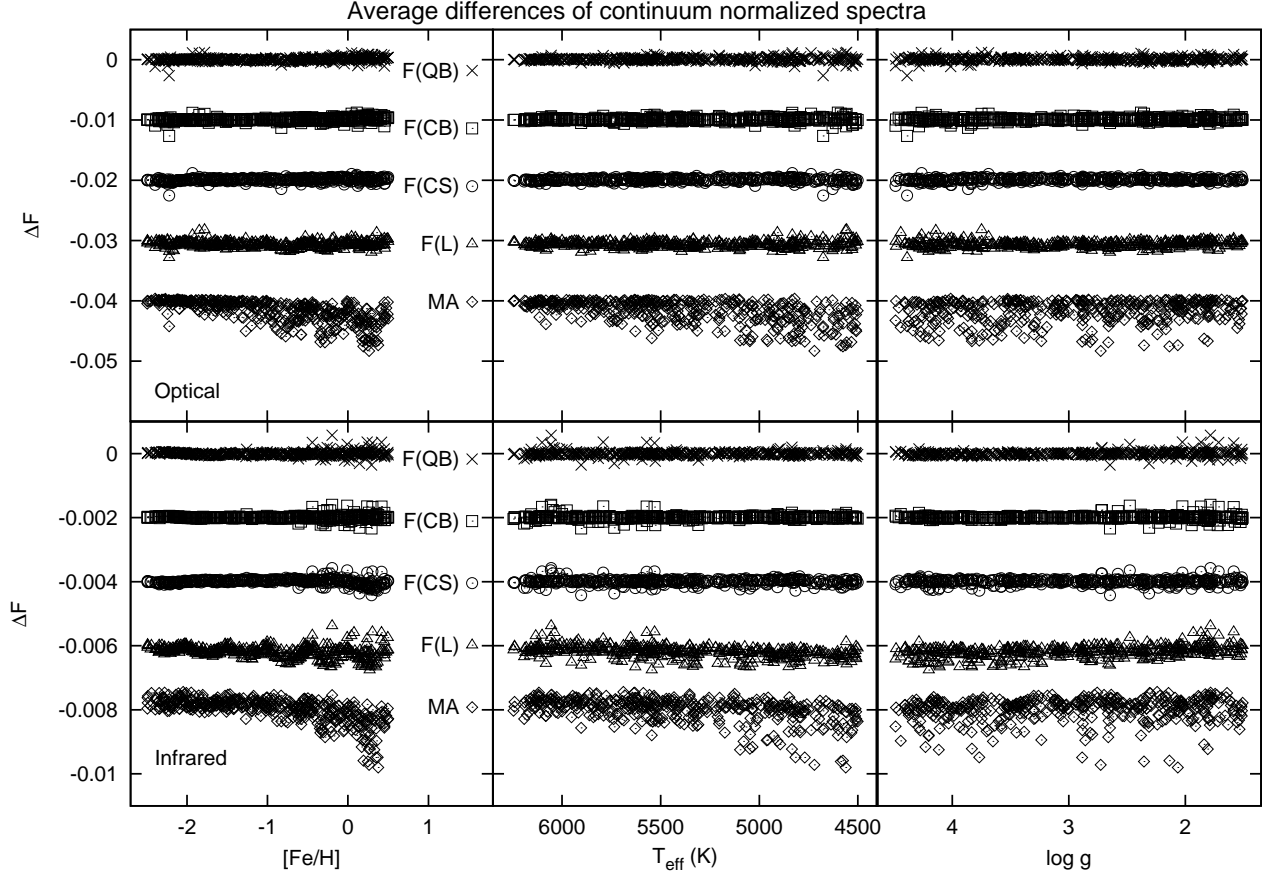


Fig. 3.— Average differences through the entire spectrum as a function of $[\text{Fe}/\text{H}]$, T_{eff} , and $\log g$. Annotations are explained in Section 2. Results for each interpolation method are shifted by 0.01, and 0.002 in optical and infrared respectively. The linear model atmosphere (MA) interpolation give significantly higher errors compared to the flux interpolations. Errors from all methods increase with increasing metallicity and decreasing temperature, however none depends on the gravity.

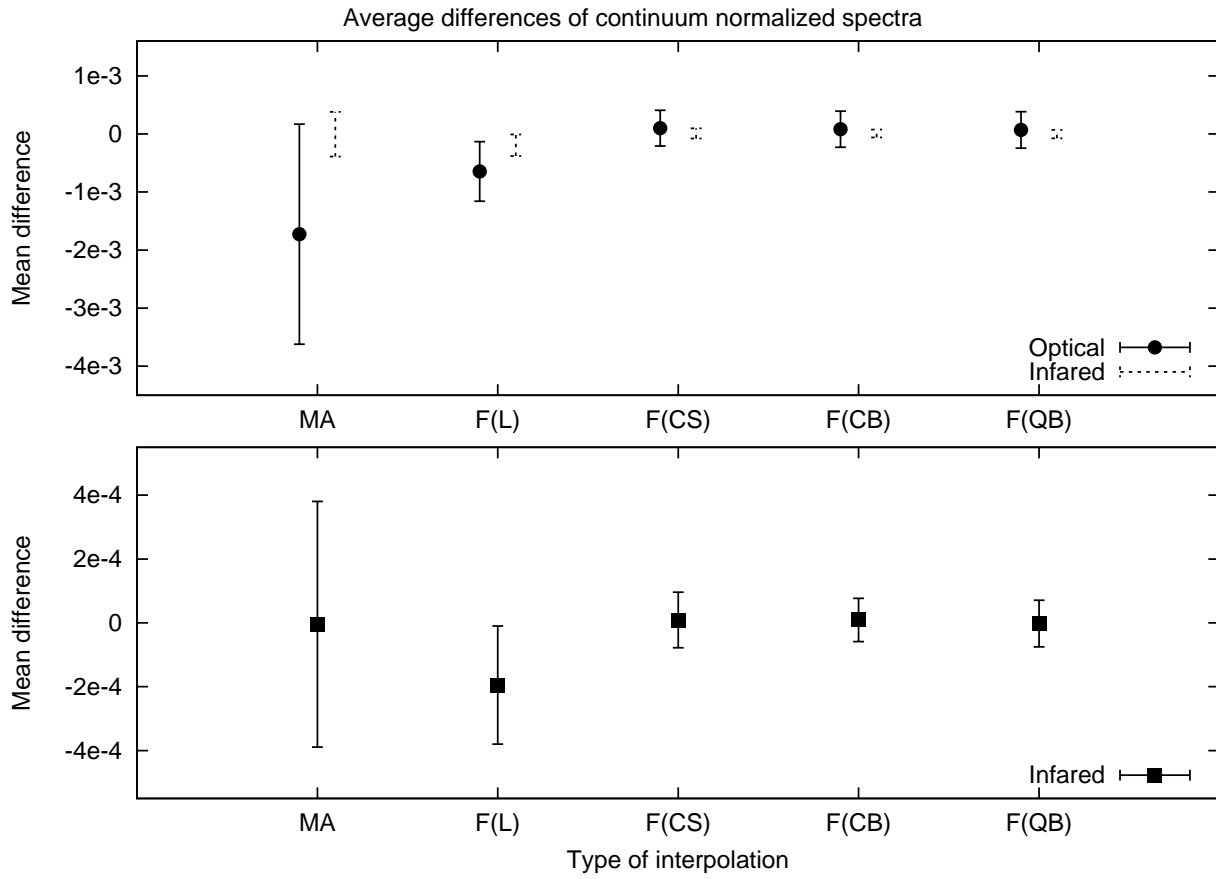


Fig. 4.— The average and standard deviation of the average relative differences of all 400 test atmosphere in continuum normalized flux for each interpolation method. Annotations are explained in Section 2. The linear model atmosphere (MA) interpolation show about a factor of 3 higher scatter than the flux interpolations, while the cubic-Bezier method gives the smoothest results.

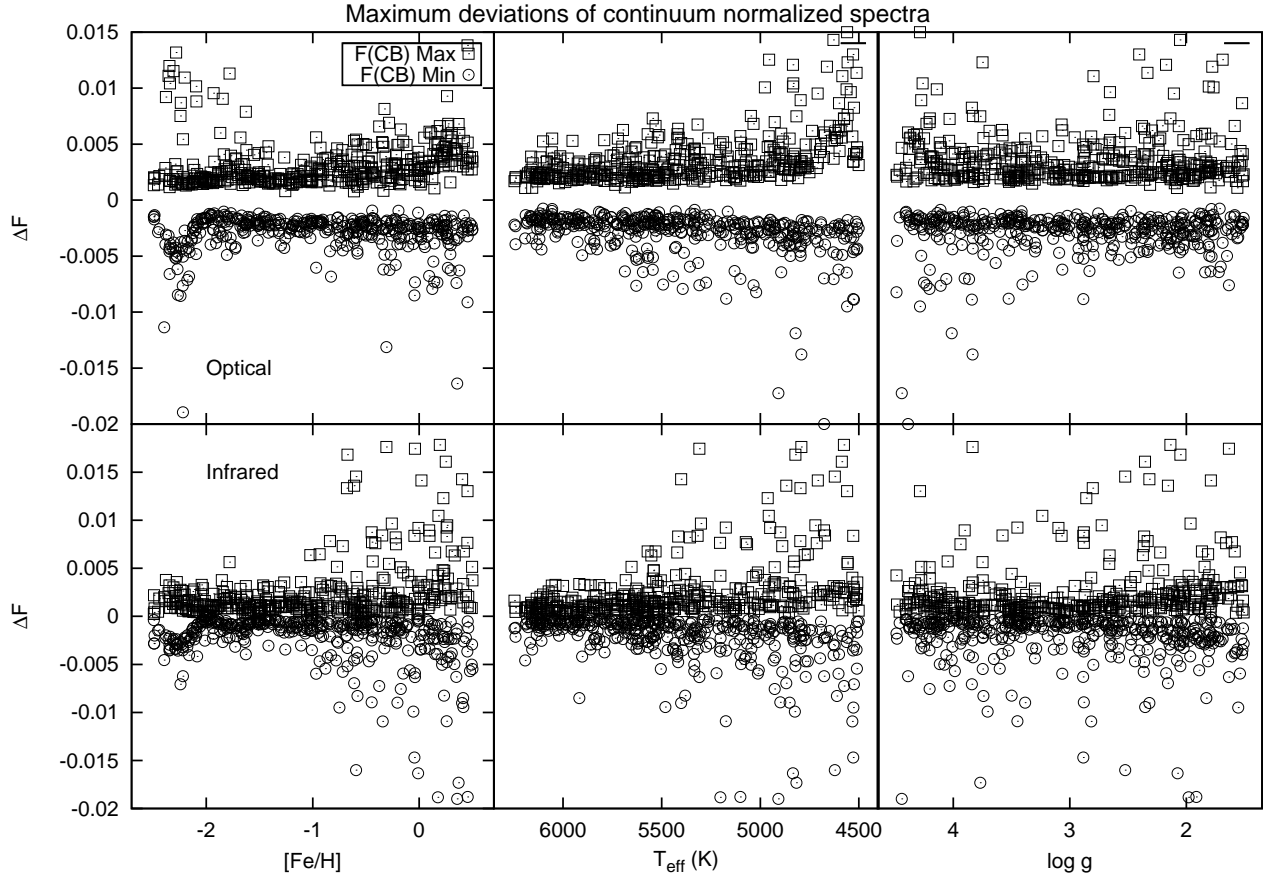


Fig. 5.— The relative maximum deviation above and below the continuum level, which tracks the largest differences in the line core profiles. Some outliers in the IR plots were not plotted to show the dependence on the physical parameters better.

Table 1. Overall statistics of all the interpolation methods

ΔF	MA	F(L)	F(CS)	F(CB)	F(QB)
Average (OP)	-1.727e-3	-6.458e-4	1.004e-4	8.263e-5	6.976e-5
S.D. (OP)	1.895e-3	5.132e-4	3.081e-4	3.103e-4	3.140e-4
Min (OP)	-0.058	-0.021	-0.018	-0.019	-0.021
Max (OP)	0.029	0.027	0.012	0.014	0.014
Average (IR)	-4.274e-6	-1.950e-4	8.928e-6	9.124e-6	-2.230e-6
S.D. (IR)	3.849e-4	1.850e-4	8.711e-5	6.775e-5	7.295e-5
Min (IR)	-0.195	-0.104	-0.108	-0.107	-0.105
Max (IR)	0.0109	0.095	0.096	0.097	0.097

Note. — OP: optical, 516.5–519.5 nm, IR: infrared, 1500–1700 nm. The type of interpolations are the following: MA: model atmosphere, F(L): linear flux, F(CS): cubic spline flux, F(CB): cubic-Bezier flux, F(QB): quadratic-Bezier flux